

# A method for delay estimation between channels of Analog to Information Converters

Bruno W. S. Arruda<sup>1</sup>, Edmar C. Gurjão<sup>2</sup>, and Raimundo C. S. Freire<sup>3</sup>

<sup>1</sup>Post-Graduation Program in Electrical Engineering - (COPELE)

<sup>2,3</sup> Department of Electrical Engineering

Federal University of Campina Grande, 58429-900, Paraíba - Brazil

e-mail: bruno.arruda@ee.ufcg.edu.br

**Abstract**— Analog signal acquisition in Compressed Sensing is implemented by Analog to Information Converters (AIC) whose physical implementation performance can be degraded due to hardware non-idealities. Methods based on comparison of the recovery of known signal with the expected output for calibration were proposed to compensate the hardware effects. However, such methods produces different results according to the recovery method. In this paper, we consider an AIC architecture composed by parallel channels and the problem of non-synchronization in channels that reduces the AIC performance. Using a controlled delay signal, we proposed a method to estimate each channel delay without the necessity of signal recovery. The results show that it is possible to measure delay in the channels of an AIC with a minimum accuracy of 1  $\mu$ s. Moreover, this method can be used in any AIC architecture composed of two or more parallel channels.

**Index Terms**— AIC; Channel; Non-synchronization; Delay; Estimation.

## I. INTRODUCTION

Compressed Sensing (CS) theory provides an approach for simultaneous signal sampling and compression, ensuring the possibility of to overcome the limits of traditional sampling based on the Shannon Theorem by exploring sparse representation of signals. Such approach avoids signal redundancy acquisition, which implies a decrease in sampling frequency compared to the Nyquist rate.

The Analog to Information Converter (AIC) is the hardware to analog signal acquisition in the Compressed Sensing. Depending on the application domain, a specific architecture is proposed [1], and utilization of AIC compared to Analog-to-Digital Converter (ADC) acquisition increases the application performance, as in Magnetic Resonance Imaging (MRI) processing [2].

Independent of architecture, the physical implementations of AIC suffer from the components imperfections and noise interference due to circuit design and fabrication [3, 4], like any device that employs mixed-signal technologies, mainly when off-the-shelf (OTS) components are used. These problems can cause, for example, gain and offset errors [5] and loss of synchronization between the input signal and the AIC control signals [6], which compromises the measurement and consequently the signal reconstruction quality. The application of a calibration process can overcome these problems improving the AIC performance.

Regarding the problem of synchronization between the input signal and the AIC control signals, some AIC calibra-

tion methods deal this problem by using sinusoids with unknown phases to estimate the frequency response of the system transfer and blind calibration using sparse recovery algorithms to estimate the delay coefficients [7, 8, 9, 10]. However, these algorithms are sensible to their input parameters and, depending on the reconstruction method, may not correspond the ideal response, which may mask effects produced by the physical characteristics of the AIC.

In this paper, we extended our previous work [6], presenting practical results and emphasizing that this delay estimation method can estimate the timing mismatch in channels of a parallel AIC implementation. The proposed method uses a copy of the sensing functions of the AIC itself and, unlike the other methods, does not depend on reconstruction algorithms.

With regards to the organization of this paper, Section II is presented an introduction to Compressed Sensing describing the fundamental aspects, the architecture of the AIC used in this paper and the experimental setup. In Section III the problem of phase error is presented. In Section IV the proposed estimation method is discussed. The results are presented in Section V and in Section VI the conclusion is presented.

## II. COMPRESSED SENSING

In simple terms, the CS framework can be expressed as the relation

$$y = \Phi x \quad (1)$$

where  $x$  is a discrete-time signal with length  $n$ ,  $\Phi$  is an  $m \times n$  sensing matrix and  $y$  is the measurement vector of length  $m$  corresponding to the compressed version of  $x$ , regarding  $m < n$ .

In eq. 1, the signal  $x$  is sparse, i.e., most of its components are equals to zero, or they can be zeroed due to their small values compared to the other signal components. If  $x$  is not sparse, it can be sparsely represented by using a sparsifying basis  $\Psi$ , i.e.,

$$x = \Psi s \quad (2)$$

where  $s = \{s_1, s_2, \dots, s_n\}$  is a sparse vector. The measurement process is now represented by

$$y = \Phi \Psi s = \Theta s. \quad (3)$$

Recovery of a signal  $x$  from the measurements  $y$  can be performed by solving the optimization problem

$$\min_s \|s\|_0 \text{ subject to } \Theta s = y, \quad (4)$$

where  $\|\cdot\|_0$  is the quasi-norm  $l_0$ , that provides the support of vector  $s$ . Such minimization permits to recover the sparse signal  $s$  with high probability, however this is a NP-hard problem. It was shown that to overcome such complexity problem the  $l_1$ -norm minimization,

$$\min_s \|s\|_1 \text{ subject to } \Theta s = y, \quad (5)$$

can be used.

To guarantee a successful recovery, matrix  $\Theta$  has to satisfy necessary and sufficient conditions, as incoherence and restricted isometry property (RIP) [11].

Analog-to-Information Converter (AIC) implements the analog signal acquisition in Compressed Sensing. In general such equipment receives a continuous-time signal  $x(t)$  and produces a discrete-time measurement vector  $y$  by projecting the input over a set of sensing functions  $\Phi$ ,  $1 \leq i \leq m$ . For the  $i$ -th component of the measurement vector  $y$

$$y_i = \int_0^T x(t) \phi_i(t) dt. \quad (6)$$

in which  $\phi_i(t)$  is the sensing function and  $T$  is the measurement period.

Some architectures implementing eq. 6 have been proposed [12]. In previous works [13, 14], we developed both a simulation model and a hardware implementation of a parallel channel AIC based on Random Modulation Pre-Integrator described as follows.

#### A. Random Modulation Pre-Integrator (RMPI)

The RMPI is a compressed sensing AIC proposed by [15], which is an ideal approach for almost all types of sparse signals. It is a parallel-channel Random Demodulator (RD), as shown in Fig. 1, taking nearly random linear combinations of samples, similar to the multiplication of the discrete-time signal  $x$  by a sensing matrix  $\Phi$  [16].

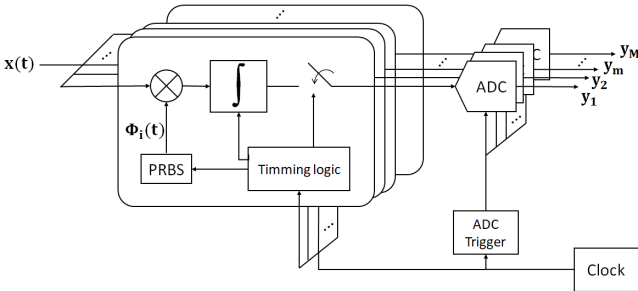


Fig. 1 Block diagram of the Random Modulation Pre-Integrator.

The analog input signal  $x(t)$  is multiplied by the  $i$ -th Pseudo-Random Binary Sequence (PRBS) and then integrated over a time window  $T$ . Then, the resulting output  $y_i$  is digitized by an ADC with sampling rate  $1/T$  conversions per unit time, which is much smaller in relation to the Nyquist rate to acquire the signal  $x(t)$  [15].

#### B. Experimental Setup

In this work, we use an 8-channel configurable RMPI, as proposed in [13, 14], composed by a digital part and an analog part, as represented in Fig. 2. The digital part consists of a Field-Programmable Gate-Array (FPGA) implementing

a Linear-Feedback Shift-Register (LFSR). The LFSR structure configuration follows a primitive polynomial, and values generated by the LFSR iterations are the PRBS of each channel [17]. Such values generate at FPGA output the sensing functions  $\phi_i$ . The FPGA also generates commands to control both measurement process (start and stop periods) and signals to reset filters. A computer stores the measurements for off-line analysis.

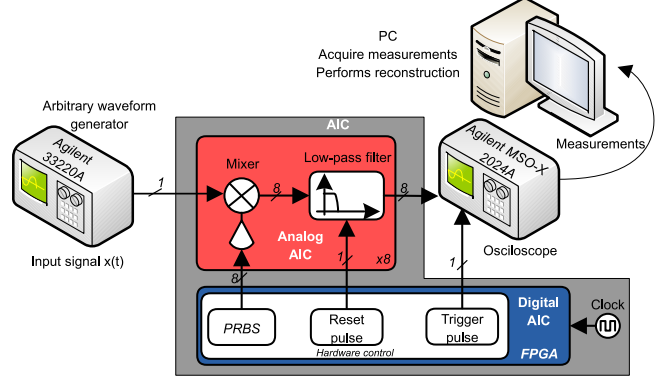


Fig. 2: Block Diagram of a RMPI based configurable analog-to-information converter based on RMPI architecture [13]

The analog part is composed by OTS components and is responsible for multiply the analog input signal  $x(t)$  by the sensing function  $\phi_i(t)$ . This hardware has 4-quadrant multipliers with a typical full-scale error of  $\pm 2\%$  and attenuation of 20 dB. After multiplication, each signal pass by an analog first order configurable low-pass filters (acting as integrators) with gain stages, where their components present tolerances between  $\pm 1\%$  and  $\pm 5\%$  and their cutoff frequencies (5 Hz, 18 Hz, 28 Hz, 50 Hz, 189 Hz, 284 Hz and 507 Hz) configured according to the desired ADC sample rate and recovery resolution [14].

A MATLAB/Simulink model of this configurable AIC implemented as described in [13] is considered as a reference of recovered signals since there is no nonlinearity or noise in the model.

### III. PROBLEM FORMULATION

Ideally, PRBS in all channels of an AIC are synchronized, i.e., the sensing functions  $\phi_i(t)$  for all channels  $i = 1, \dots, m$  start at the same instant  $t$  and range all  $N$  periods of the sensing function. However, due to hardware non-idealities, one or more sequences can have a delay. This is represented in Fig. 3, where  $x(t)$  is the input signal and  $\phi_i(t)$  is a sensing function composed by a sequence of square pulses with amplitudes  $\pm 1$  delayed by  $\Delta_i$ . This behavior on the  $i$ -th channel measurement can be modeled as

$$\hat{y}_i = \int_0^T x(t) \phi_i(t - \Delta_i) dt, \quad (7)$$

where  $\Delta_i$  represents the delay in the  $i$ -th channel. When providing the sensing matrix ( $\Phi$ ) and the measurement vector ( $y$ ) to a reconstruction algorithm that solves the eq. 5, signal reconstruction will be degraded due to sensing matrix mismatch the practical one.

Using the MATLAB/Simulink model of the RMPI described in Section II, a constant delay  $\Delta$  defined as a frac-

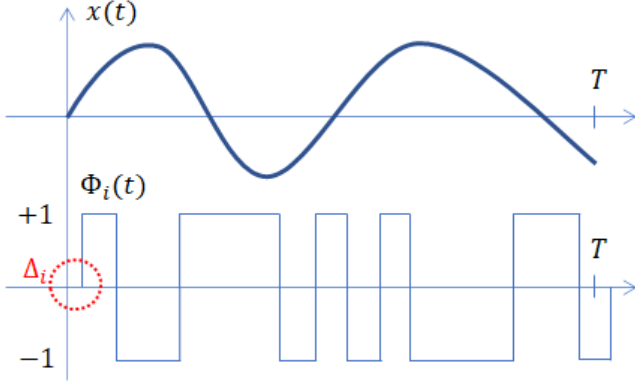


Fig. 3: Synchronism problem between AIC signals: sensing function delayed by  $\Delta$  with respect to the input signal.

tion of the PRBS period  $T_{PRBS}$  was introduced in all channels. Simulating this scenario with parameters presented in Table I, the effect of delay was evaluated by Signal-to-Noise and Distortion Ratio (SINAD) [18, 19] of obtained measurement values, as shown in Fig. 4.

Table I. Parameters set up on SINAD simulation.

Parameter	Value
Input signal	Sinusoid
Input signal amplitude	$1 V_{pp}$
Input signal frequency	$1 kHz$
Primitive polynomial (PRBS)	$x^5 + x^3 + x^2 + x + 1$
Measurement matrix dimension ( $M \times N$ )	$8 \times 32$
Low-pass filter cutoff frequency	$\approx 50 Hz$

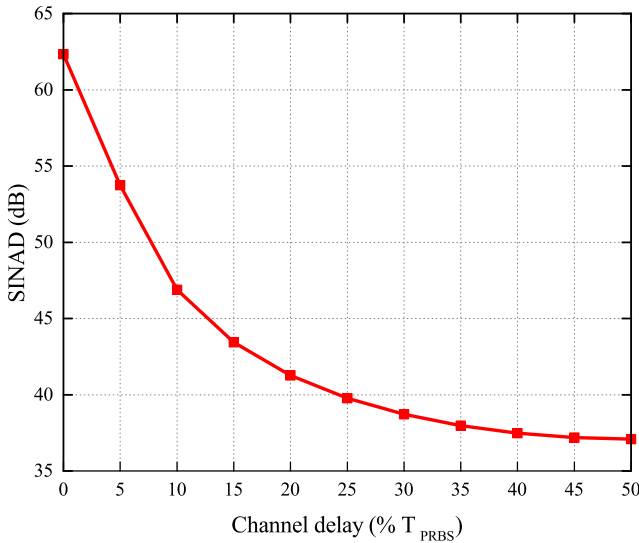


Fig. 4 SINAD behavior according to channel delay.

A null channel delay implies synchronization in all channels, while as  $\Delta_i$  increases SINAD decreases exponentially, which demonstrates the negative effect of delay on AIC performance. To avoid the distorted measurement ends up leading to inadequate reconstruction of the input signal, the value of  $\Delta_i$  must be estimated in order to compensate the measurement.

#### IV. PROPOSED ESTIMATION METHOD

To estimate the channel delay  $\Delta_i$ , we propose a method based on an indirect measurement, using a known and con-

trollable input signal. The correlation between this input signal  $x(t)$  and the sensing function in each channel  $\phi_i(t)$  is analyzed. In this case, to obtain a correlation value, the input signal becomes a copy of the sensing function  $\phi_i(t)$  with controlled phase (delay)  $\tau$ , that is,  $\phi_i(t - \tau)$ . Thus, the measurement of the  $i$ -th channel, which is the correlated value of the two signals, is given by

$$\hat{y}_i = \int_0^T \phi_i(t - \tau) \phi_i(t - \Delta_i) dt. \quad (8)$$

Analyzing Equation 8, it can be noticed that by varying the parameter  $\tau$ ,  $\hat{y}_i$  will have the maximum value when  $\tau$  is equals to  $\Delta_i$ . In this case, the expected value of the measurement  $\hat{y}_i$  will be numerically equals to  $T$ , when both signals present the highest level of correlation with each other (assuming that all measurements have an initial value equal to zero). In practice, however,  $\hat{y}_i$  will not be numerically equals to  $T$ , as the integrators are not ideal. As proof of concept, let's consider a simulation of the AIC described in Section II, performing measurement of a signal  $x(t)$ , according to the parameters described in Table II, assuming all sensing functions  $\phi_i(t)$  being equal to  $x(t)$  as shown in eq. 8 and that all AIC channels have an unknown  $\Delta_i$  delay.

Table II. Parameters set up on simulation/hardware.

Parameter	Value
Input signal	Pulse
Input signal amplitude	$2 V_{pp}$
Input signal frequency	$1 kHz$
Duty cycle	50 %
Low-pass filter cutoff frequency	$\approx 50 Hz$

To estimate the delay of each channel, we vary phase  $\tau$  of  $x(t)$  between 0 s and 50% of  $T_{PRBS}$  and observed the values of  $\hat{y}_i$ . Fig. 5 shows the measurement values of each channel obtained by simulation according to channel delay  $\tau$ , as well as the ideal value for perfect synchronization between signals. It is important to notice that for the ideal case in this simulation scenario, the measurement value is 1.72 V for all channels.

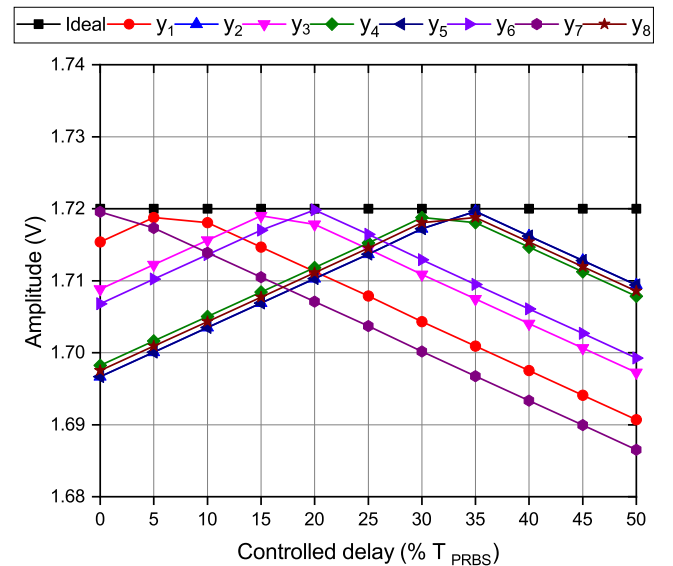


Fig. 5 Correlation values between input signal and measurement signals

It can be seen that the maximum value of the measurement occurs when the controlled delay  $\tau$  is as close as possible to  $\Delta_i$ , i.e., the channel delay is estimated according to the first curve peak. However, for better accuracy, it is necessary to decrease the variation step of the controlled delay, so that when  $\tau = \Delta_i$ , the measurement  $\hat{y}_i$  reflects the maximum correlation. In this way, this method can be applied to obtain an estimate of the delay in each channel of the AIC, and the values obtained can be used to compensate the measurements during the signal reconstruction step.

## V. EXPERIMENTAL RESULTS

In order to evaluate the proposed method, simulations and hardware experiments were performed based on the parameters presented in Table II. We set a delay  $\Delta_i$  of  $5 \mu s$  on each of the 8 channels of the AIC and simulated a sweep of  $\tau$  values from 0 to  $10 \mu s$  (steps of  $1 \mu s$ ), to obtain a reference curve for the hardware experiment. Fig. 6 shows the behaviour of the measurements  $\hat{y}_i$  in function of  $\tau$ .

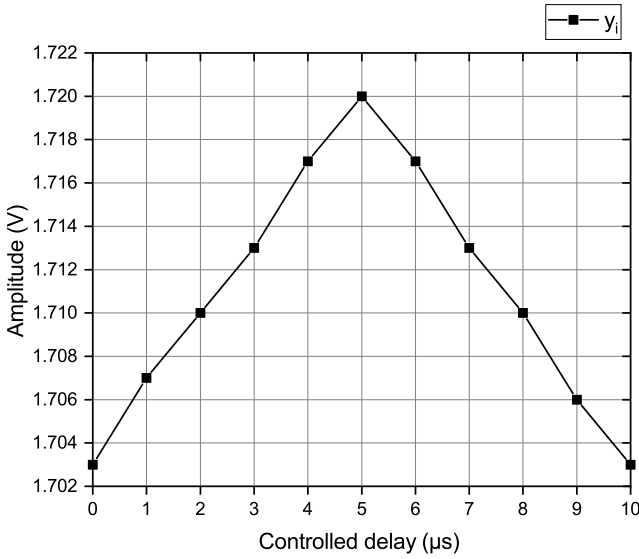


Fig. 6: Measurement values of the  $i$ -channel versus the variation of controlled delay ( $\tau$ ) of the input signal.

It can be noticed the peak value of the measurement occurs exactly when the controlled delay  $\tau$  is equal to  $\Delta_i$ , i.e., as the phase of the input signal approaches the delay inherent in the channel, the measurement value reaches its maximum value. In contrast, when the input signal phase is greater than channel delay, the measured value decreases.

In hardware, the measurement value was also obtained in function of the controlled delay  $\tau$ . It is worth notice that in this measurement, gain and offset errors arising from hardware non-idealities also become visible and it is necessary to attenuate them. Fig. 7 shows the values of measurements without compensation compared to the expected ideal values. By means of gain and offset errors calibration/compensation method proposed in [5], we compensated the measurements, as can be seen in Fig. 8.

In Fig. 7 it is possible to clearly observe the influence of gain and offset errors, making it difficult to quantify the difference in relation to the ideal behavior of the measurement. With compensated gain and displacement errors, as can be seen in Fig. 8, it is possible to observe that the effects

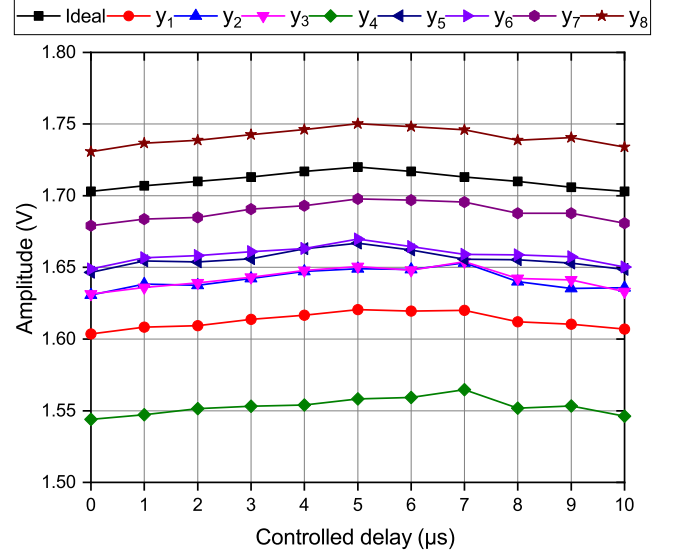


Fig. 7: Measurement values in 8 AIC channel and ideal measurement (simulation) without compensated measurements.

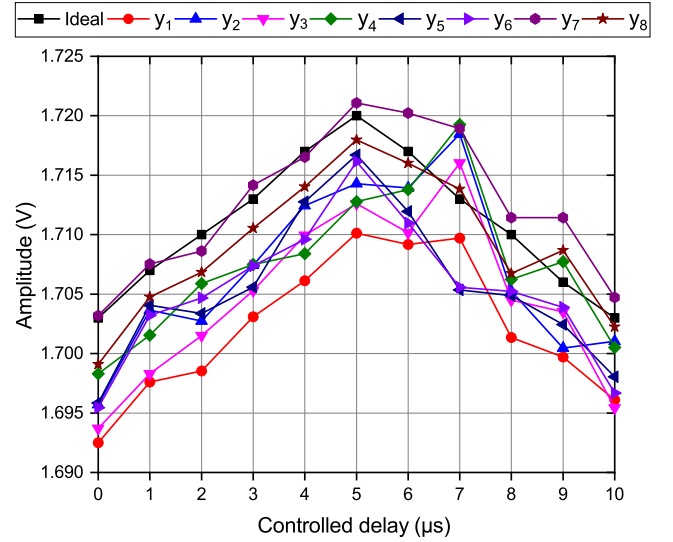


Fig. 8: Measurement values in 8 AIC channel and ideal measurement (simulation) with compensated measurements.

caused by these errors are mitigated and there is a tendency towards the expected behavior of the measurements, showing, on most channels, maximum value when the controlled delay is  $5 \mu s$ .

In another perspective, in Fig. 8, it can be noticed that the values present a certain variation in the ideal trend. This can be explained by the influence of noise on the measurement, since this method is performed using a low amplitude signal. Furthermore, it is possible to observe that in some channels the maximum value of the measurement happens at  $7 \mu s$ , which can be justified by the natural delay of each channel and by the measurement noise. It is worth remembering that a delay of  $5 \mu s$  was configured on each channel, however, as the hardware, by definition, is not ideal, there is no guarantee that each channel may present a natural delay. Despite this, in a situation where the influence of noise is minimal, the important thing to note is the first peak of the measurement. Considering a real situation in which the delay is different for all channels, each one must be analyzed individually in order

to make a correct estimate, avoiding that in the reconstruction of the compensated measurement it is a time-shifted version of the input signal, which can cause the effect shown in Fig. 4.

## VI. CONCLUSION

In this paper, a delay estimation in channels of AIC method was presented. Unlike other estimation methods presented in the literature, the proposed method does not rely on using sinusoids with unknown phases to estimate the frequency response of the system transfer and blind calibration using sparse reconstruction algorithms, since it obtains delay values before signal reconstruction. It is possible to provide these values for any compensation method, so that the effect of the reconstruction algorithms is removed. The obtained results demonstrate that it is possible to estimate the delay of each channel without the use of reconstruction algorithms, matrix manipulations and test signals [7, 8], using a simple and easy-to-implement approach. However, it is still necessary to carry out further studies on how to use these estimated values in the measurement compensation, so that the method can be better evaluated with, for example, figures of merit. In another way, it is worth mentioning that although the whole procedure is mathematically simple, it is necessary to control the phase of the input signal and, depending on the number of AIC channels and the desired accuracy, it can take a long time.

## ACKNOWLEDGEMENTS

The authors would like to thank CAPES, PRONEX/FAPESQ and CNPq for the support and funding.

## REFERENCES

- [1] M. Rani, S. B. Dhok, and R. B. Deshmukh, "A systematic review of compressive sensing: Concepts, implementations and applications," *IEEE Access*, vol. 6, pp. 4875–4894, 2018.
- [2] J. Hutter, R. Grimm, C. Forman, A. Greiser, J. Hornegger, and P. Schmitt, "Multi-dimensional flow-adapted compressed sensing (mdfcs) for time-resolved velocity-encoded phase contrast mra," in *2013 IEEE 10th International Symposium on Biomedical Imaging*, 2013, pp. 13–16.
- [3] Y. Zhao, H. Wang, Y. Zheng, Y. Zhuang, and N. Zhou, "High sampling rate or high resolution in a sub-nyquist sampling system," *Measurement*, vol. 166, p. 108175, 2020. [Online]. Available: <https://www.sciencedirect.com/science/article/pii/S0263224120307132>
- [4] C. A. Reis, "Review of offset and noise reduction techniques for cmos," *Journal of Integrated Circuits and Systems*, vol. 17, no. 1, 2022. [Online]. Available: <http://dx.doi.org/10.29292/jics.v17i1.572>
- [5] B. W. S. Arruda, R. C. S. Freire, E. C. Gurjão, V. M. L. Lima, and V. Reis, "Gain and offset calibration for an analog-to-information converter," in *2018 3rd International Symposium on Instrumentation Systems, Circuits and Transducers (INSCIT)*, Aug. 2018, pp. 1–5.
- [6] B. W. S. Arruda, E. C. Gurjão, L. F. N. M. Torres, V. L. Reis, and R. C. S. Freire, "Estimation of channel delay in analog-to-information converters," in *2019 IEEE International Symposium on Circuits and Systems (ISCAS)*, 2019, pp. 1–4.
- [7] J. Park, J. Jang, and H. Lee, "A calibration for the modulated wideband converter using sinusoids with unknown phases," in *2017 Ninth International Conference on Ubiquitous and Future Networks (ICUFN)*, 2017, pp. 951–955.
- [8] N. Dong and J. Wang, "Channel gain mismatch and time delay calibration for modulated wideband converter-based compressive sampling," *IET Signal Processing*, vol. 8, no. 2, pp. 211–219, 2014. [Online]. Available: <https://ietresearch.onlinelibrary.wiley.com/doi/abs/10.1049/iet-spr.2013.0137>
- [9] Y. Li, K. Lee, and Y. Bresler, "Blind gain and phase calibration for low-dimensional or sparse signal sensing via power iteration," in *2017 International Conference on Sampling Theory and Applications (SampTA)*, July 2017, pp. 119–123.
- [10] S. J. Wijnholds and S. Chiarucci, "Blind calibration of phased arrays using sparsity constraints on the signal model," in *2016 24th European Signal Processing Conference (EUSIPCO)*, 2016, pp. 270–274.
- [11] E. J. Candes and T. Tao, "Near-Optimal Signal Recovery From Random Projections: Universal Encoding Strategies?" *IEEE Transactions on Information Theory*, vol. 52, no. 12, pp. 5406–5425, Dec. 2006.
- [12] M. Mangia, F. Pareschi, V. Cambareri, R. Rovatti, and G. Setti, *Adapted Compressed Sensing for Effective Hardware Implementations: A Design Flow for Signal-Level Optimization of Compressed Sensing Stages*. Springer, Jul. 2017, google-Books-ID: gdk5D-wAAQBAJ.
- [13] V. L. Reis, E. C. Gurjão, and R. C. S. Freire, "Using synchronism pulse to improve A2i implementations," in *2015 IEEE International Instrumentation and Measurement Technology Conference (I2MTC) Proceedings*, May 2015, pp. 13–17.
- [14] V. L. Reis, P. C. Lobo, E. C. Gurjão, and R. C. S. Freire, "Influence of integrators in the performance of analog-to-information converters," in *2016 1st International Symposium on Instrumentation Systems, Circuits and Transducers (INSCIT)*, Aug. 2016, pp. 118–121.
- [15] J. Yoo, S. Becker, M. Monge, M. Loh, E. Candès, and A. Emami-Neyestanak, "Design and implementation of a fully integrated compressed-sensing signal acquisition system," in *2012 IEEE International Conference on Acoustics, Speech and Signal Processing (ICASSP)*, 2012, pp. 5325–5328.
- [16] M. Wakin, S. Becker, E. Nakamura, M. Grant, E. Sovero, D. Ching, J. Yoo, J. Romberg, A. Emami-Neyestanak, and E. Candes, "A nonuniform sampler for wideband spectrally-sparse environments," *IEEE Journal on Emerging and Selected Topics in Circuits and Systems*, vol. 2, no. 3, pp. 516–529, Sept 2012.
- [17] B. W. S. Arruda, R. C. S. Freire, L. F. N. M. Torres, V. L. Reis, and E. C. Gurjão, "Influence of measurement matrix characteristics in a configurable analog-to-information converter performance," in *2017 2nd International Symposium on Instrumentation Systems, Circuits and Transducers (INSCIT)*, Aug 2017, pp. 1–4.
- [18] P. Daponte, L. D. Vito, and S. Rapuano, "An extension to IEEE Std. 1241 sine fit for analog-to-information converters testing," in *2015 IEEE International Instrumentation and Measurement Technology Conference (I2MTC) Proceedings*, May 2015, pp. 1933–1937.
- [19] V. M. L. Silva, B. W. S. Arruda, C. P. de Souza, E. C. Gurjão, V. L. Reis, and R. C. S. Freire, "A testing approach for a configurable rmp-based analog-to-information converter," in *2018 IEEE International Instrumentation and Measurement Technology Conference (I2MTC)*, May 2018, pp. 1–5.